Who Moved My Distribution? Conformal Prediction for Interactive Multi-Agent Systems

Allen Emmanuel Binny

ALLENEBINNY@KGPIAN.IITKGP.AC.IN

Department of Electronics and Electrical Communication Engineering, IIT Kharagpur, India

Anushri Dixit Anushridixit@ucla.edu

Department of Mechanical and Aerospace Engineering, University of California, Los Angeles, USA

Abstract

Uncertainty-aware prediction is essential for safe motion planning, especially when using learned models to forecast the behavior of surrounding agents. Conformal prediction is a statistical tool often used to produce uncertainty-aware prediction regions for machine learning models. Most existing frameworks utilizing conformal prediction-based uncertainty predictions assume that the surrounding agents are non-interactive. This is because in closed-loop, as uncertainty-aware agents change their behavior to account for prediction uncertainty, the surrounding agents respond to this change, leading to a distribution shift which we call *endogenous distribution shift*. To address this challenge, we introduce an iterative conformal prediction framework that systematically adapts the uncertainty-aware ego-agent controller to the endogenous distribution shift. The proposed method provides probabilistic safety guarantees while adapting to the evolving behavior of reactive, nonego agents. We establish a model for the endogenous distribution shift and provide the conditions for the iterative conformal prediction pipeline to converge under such a distribution shift. We validate our framework in simulation for 2- and 3- agent interaction scenarios, demonstrating collision avoidance without resulting in overly conservative behavior and an overall improvement in success rates of up to 9.6% compared to other conformal prediction-based baselines.

Keywords: Conformal prediction, model predictive control, multi-agent systems, trajectory forecasting, safe planning

1. Introduction

Modern learning-based methods have demonstrated impressive capabilities in predicting multiagent trajectories. These include architectures such as long short-term memory (LSTM) networks (Rhinehart et al. (2019); Alahi et al. (2016); Salzmann et al. (2021)), diffusion models (Samavi et al. (2025)), and transformers (Shi et al. (2022); Yuan et al. (2021)). For self-driving applications, trajectory predictors are typically trained on data collected from simulators, such as CARLA (Dosovitskiy et al. (2017)), or large-scale datasets, such as the Waymo Open Dataset (Chen et al. (2024)). However, these predictors cannot provide safety guarantees for collision avoidance and are susceptible to poor performance under distribution shifts when encountering previously unobserved data, potentially leading to catastrophic failures (Fields (2025)). Hence, we need uncertainty quantification tools that can provide safety and reliability guarantees for learning-based trajectory predictors. We employ conformal prediction (CP), a statistical tool introduced by Vovk et al. (2005) to provide formal guarantees with user-specified probability $1 - \epsilon$ for navigation alongside reactive agents. While previous methods by Kuipers et al. (2024); Lindemann et al. (2023); Dixit et al. (2023) have introduced CP techniques for safe multi-agent interactions where the policies of the other, non-ego agents are not allowed to change, we uniquely establish a method for multi-agent CP where the

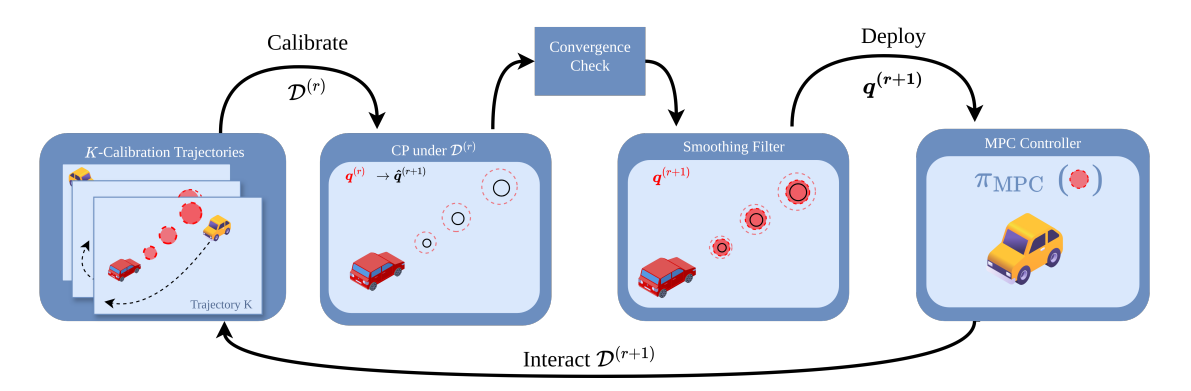


Figure 1: *Iterative Conformal Prediction Framework Overview:* The process alternates between calibration using collected agent trajectories, updating and smoothing the conformal prediction sets, and deploying an uncertainty-aware controller, with iterative adaptation until convergence is reached under endogenous distribution shift.

non-ego agents can have policies similar to the ego agent and are allowed to respond to changes in the ego agent's behavior.

Incorporating uncertainty predictions into learning-based decision-making in environments with other reactive agents introduces new challenges. Typically, the learned trajectory prediction module is trained with uncertainty-agnostic controllers. Consequently, deploying an uncertainty-aware controller results in a distribution shift, as other agents adjust their behavior in response to changed ego agent behavior (from an uncertainty-agnostic policy to uncertainty-aware policy). We refer to this phenomenon as endogenous distribution shift, which remains largely unaddressed in existing safe motion planning frameworks. Our motivation stems from two sources: 1) the concept of closed-loop distribution shift described introduced by Mei et al. (2025), where the closed-loop deployment of an uncertainty-quantified perception system combined with a safe planner causes a shift in the state distribution, and 2) the method of performative prediction developed by Perdomo et al. (2020) to study the influence of predictive models on the outcomes they aim to predict. Building on these two threads, we provide a multi-agent CP framework that can adapt to endogenous distribution shifts instead of being robust to distribution shifts like Mei et al. (2025). The work by Mei et al. (2025) also provides safety guarantees only for static environments (without other agents) and requires the use of a sampling-based safe planner. Our work addresses performativity for multi-agent decisionmaking by adapting the framework by Perdomo et al. (2020) to CP-based multi-agent planning. The main contributions of this paper are:

- We introduce a model for endogenous distribution shift in uncertainty-aware motion planning, where closed-loop deployment of CP-based predictions alters the data distribution of the interactions between agents and undermines the performance of the controller.
- We propose an iterative CP algorithm (as demonstrated in Figure 1) integrated with model predictive control (MPC) that recalibrates prediction regions using trajectory data collected under the deployed controller, providing probabilistic safety guarantees while accounting for endogenous distribution shifts in reactive multi-agent settings.
- We provide theoretical insights for the convergence of our iterative CP algorithm under mild Lipschitzness assumptions.
- We demonstrate our results through experiments in a multi-agent environment simulation and compare them to the benchmarks of cases without the iterative framework of CP.

2. Preliminaries

Trajectory Prediction: Given observations (Y_0,\ldots,Y_t) at time t, we want to predict future states (Y_{t+1},\ldots,Y_{t+H}) for a prediction horizon of H. Assume that $\operatorname{TrajPred}$ is a function that maps observations (Y_0,\ldots,Y_t) to predictions $(\hat{Y}_{t+1|t},\ldots,\hat{Y}_{t+H|t})$. Note that t in $\hat{Y}_{t+\tau|t}$ denotes the time at which the prediction is made, while τ indicates how many steps we predict ahead. To obtain multi-step predictions, the model is rolled out recursively: the predicted $\hat{Y}_{t+1|t}$ is fed back as input to predict $\hat{Y}_{t+2|t}$, and so on, up to horizon H. While our framework is compatible with any trajectory predictor, in practice, we adopt recurrent neural networks (RNNs) (Hochreiter and Schmidhuber (1997)), specifically long short-term memory (LSTM) models, due to their ability to capture nonlinear and long-term dependencies.

Conformal Prediction: Conformal prediction (CP) (Vovk et al. (2005); Angelopoulos et al. (2025)) will be our primary tool for performing rigorous uncertainty quantification for trajectory prediction. Given K i.i.d. (or exchangeable) samples U_1, \ldots, U_K of a scalar random variable U, we compute the threshold, $\hat{q}_{1-\epsilon}$, such that the next sample, U_{test} , satisfies,

$$\mathbb{P}[U_{\text{test}} \le \hat{q}_{1-\epsilon}] \ge 1 - \epsilon,\tag{1}$$

$$\hat{q}_{1-\epsilon} = \begin{cases} U_{(\lceil (K+1)(1-\epsilon) \rceil)} & \text{if } \lceil (K+1)(1-\epsilon) \rceil \le K, \\ \infty & \text{otherwise,} \end{cases}$$
 (2)

and $U_{(1)} \leq U_{(2)} \leq \ldots \leq U_{(K)}$ are the order statistics (sorted values) of the K samples U_1,\ldots,U_K . In the CP literature, U is known as the non-conformity score and it is a measure of the (in)correctness of a model. The above guarantee is marginal, i.e., it holds over the sampling of both the calibration dataset U_1,\ldots,U_K and the test variable U_{test} . Hence, we need to generate a fresh set of i.i.d. calibration data U_1,\ldots,U_K for the guarantee to hold for a new sample U_{test} . However, in practice, one typically only has access to a single dataset of examples; inferences from this dataset must be used for all future predictions on test examples. In this work, we use the following dataset-conditional guarantee (Vovk (2012); Angelopoulos and Bates (2022)) that does not require us to generate K new samples for every test prediction and holds with probability $1-\delta$ over the sampling of the calibration dataset,

$$\mathbb{P}[U_{\text{test}} \le \hat{q}_{1-\epsilon}|U_1, \dots, U_K] \ge \text{Beta}_{K+1-v,v}^{-1}(\delta), \tag{3}$$

where, $v:=\lfloor (K+1)\epsilon \rfloor$, and $\operatorname{Beta}_{K+1-v,v}^{-1}(\delta)$ is the δ -quantile of the Beta distribution with parameters K+1-v and v. We can choose ϵ to achieve the desired $1-\epsilon$ coverage.

Notation: The system operates with N other dynamic agents whose trajectories are apriori unknown. We define an iterate r, for which $\mathcal{D}^{(r)}$ denotes an unknown distribution over agent trajectories collected at that iteration. We sample an interaction between agents by sampling a random trajectory $Y^{(r)} := (Y_0^{(r)}, Y_1^{(r)}, \dots) \sim \mathcal{D}^{(r)}$ where the joint agent state at time t is given by $Y_t^{(r)} := (Y_{t,0}^{(r)}, \dots, Y_{t,N}^{(r)}) \in \mathbb{R}^{(N+1)\times n}$, i.e., $Y_{t,j}$ is the state of agent j at time t (agent 0 is used to denote the ego agent). During the calibration phase, for each iteration r, we form a dataset of K interaction trajectories, $D_{cal}^{(r)} := \{Y^{(r),1}, \dots, Y^{(r),K}\}$ in which each of the K trajectories are exchangeable and $Y^{(r),i} := \{Y_0^{(r),i}, Y_1^{(r),i}, \dots\} \sim \mathcal{D}^{(r)}$. For simplicity, sometimes we drop the notation for each iteration r when the same algorithm is applied for all the iterations in the same way,

^{1.} We assume the state of each agent to be n-dimensional. This can easily be generalized.

i.e., $Y^{(r)}$ is sometimes denoted as Y. Similarly, for the rest of the paper, we consider the two agent case, i.e., N=1, but our results hold for any N>1. The same notation is used for predicted trajectories, but instead of Y, we denote predicted trajectories by \hat{Y} . We denote, $\mathcal{D}^*:=\lim_{r\to\infty}\mathcal{D}^{(r)}$ and $Y^*:=\lim_{r\to\infty}Y^{(r)}$.

3. Problem Statement

3.1. System Dynamics and Environment

We consider an (ego) agent governed by the discrete-time dynamics,

$$x_{t+1} = f(x_t, u_t), \qquad x_0 = x(0),$$
 (4)

with state $x_t \in \mathcal{X} \subseteq \mathbb{R}^n$ and control input $u_t \in \mathcal{U} \subseteq \mathbb{R}^m$ at time t. The sets \mathcal{X} and \mathcal{U} denote state and input constraints, respectively, $f: \mathcal{X} \times \mathcal{U} \to \mathcal{X}$ describes the dynamics, and $x(0) \in \mathbb{R}^n$ is the initial condition.

The ego agent navigates an environment with N other dynamic agents (we present the N=1 case for simplicity) that can plan and react to the behavior of the other agents in a decentralized manner. Within its motion planning framework, each agent predicts other agents' locations using any learned trajectory predictor module, TrajPred (Salzmann et al. (2021); Alahi et al. (2016)). In this work, we aim to make uncertainty-aware predictions on the behavior of such reactive agents so that we can provide statistical assurances for the safety of the system (4) without any information about the dynamics and control of the dynamic agents in the environment. We utilize a model predictive control (MPC) strategy with cost J and prediction horizon H to ensure safety,

$$\pi_{\text{MPC}}(\boldsymbol{d}_{\min}) = \min_{(u_{t|t}, \dots, u_{t+H-1|t})} \sum_{\kappa=0}^{H-1} J(x_{t+\kappa+1|t}, u_{t+\kappa|t})$$
 (5a)

s.t.
$$x_{t+\kappa|t} = f(x_{t+\kappa-1|t}, u_{t+\kappa-1|t}),$$
 (5b)

$$c(x_{t+\kappa|t}, \hat{Y}_{t+\kappa|t}) \ge d_{\min,\kappa},$$
 (5c)

$$u_{t+\kappa|t} \in \mathcal{U}, x_{t+\kappa+1|t} \in \mathcal{X},$$
 (5d)

$$x_{t|t} = x(t), (5e)$$

where, $x_{t+\kappa|t}, u_{t+\kappa|t}$ describe the state and control predicted for time $t+\kappa$ at time t for $\kappa \in \{1,\ldots,H\}$, and $\hat{Y}_{t+\kappa|t}$ describes the H-step predicted trajectories of each of the N other agents at time t using TrajPred. The collision avoidance safety constraint is described by the function c that measures the predicted distance between the ego agent state $x_{t+\kappa|t}$ and that of the other agents in the scene, i.e., $c(x_{t+\kappa|t}, \hat{Y}_{t+\kappa|t}) = \|x_{t+\kappa|t} - \hat{Y}_{t+\kappa|t}\|_2$.

Based on the accuracy of TrajPred, the predicted states of the other agents, $\hat{Y}_{t+\kappa|t}$, may be imperfect. To ensure the safety of the ego agent, we quantify the uncertainty associated with TrajPred using an uncertainty-aware collision threshold, $d_{\min,\kappa} = \hat{q}_{\kappa}$ using CP. We assume that we have access to a calibration dataset of i.i.d. interactions between all agents. We compute the prediction error $U = \|Y - \hat{Y}\|$ using the actual realized trajectory of the agents, Y and the predicted trajectory, \hat{Y} , to estimate a statistically valid $\mathbf{q} = [q_1, \dots, q_H]^T$. For simplicity, we consider that the other N agents utilize an MPC planner $\pi_{\mathrm{MPC}}(\mathbf{0})$. However, this can be generalized to another planner with obstacle avoidance, such as using control barrier functions (Ames et al. (2017)) or dynamic window approach (Fox et al. (1997)).

3.2. Endogenous Distribution Shifts

When collecting the initial calibration dataset, we utilize a nominal controller without any uncertainty-aware constraint tightening, i.e., $\pi_{\text{MPC}}(\mathbf{0})$ with $d_{\min} = \mathbf{0}$. We then estimate the desired tightening $d_{\min} = q$ using CP (defined in section 4.2) leading to a new, uncertainty-aware policy, $\pi_{\text{MPC}}(q)$ that is reliable and safe for any environment drawn from the distribution $\mathcal{D}^{(0)}$ with the desired probability. Since other agents in the environment have reactive policies, their behaviors will now change in response to the new policy leading to an unknown distribution shift in the interaction trajectories $\mathcal{D}^{(0)} \to \mathcal{D}$. We define this distribution shift caused by internal changes to the system controller endogenous distribution shift. Our goal in this work is to ensure the safety of the ego agent in such a dynamic and shifting environment without comprising on the performance of the controller.

Problem 1 Consider the discrete-time dynamical system given in (4) with a control law governed by $u = \pi_{MPC}(\mathbf{0})$ that accounts for the motion of other unknown agents in the environment, $Y_t^{(0)} \sim \mathcal{D}^{(0)}$ using a learned trajectory predictor, TrajPred. Compute a constraint tightening, \mathbf{q}^* associated with a stable, non-shifting distribution \mathcal{D}^* , such that $\pi_{MPC}(\mathbf{q}^*)$ is safe with probability $1 - \epsilon$ with,

$$\mathbb{P}\left(\|Y_{t+\kappa}^* - \hat{Y}_{t+\kappa|t}\| \le q_{\kappa}^*\right) \ge 1 - \epsilon, \quad \forall \kappa \in \{1, \dots, H\},\tag{6}$$

where, the realized agent interactions under the control law $\pi_{MPC}(q^*)$ satisfy $Y_{t+\kappa}^* \sim \mathcal{D}^*$ and $Y_{t+\kappa}^* - \hat{Y}_{t+\kappa|t}$ is the difference between the actual trajectories of all agents at time $t + \kappa$ and the predicted trajectories as predicted by TrajPred at time t with failure probability $\epsilon \in [0,1)$.

4. Conformal Prediction under Endogenous Distribution Shift

We now describe our iterative conformal prediction framework to adapt the CP-based uncertainty predictions to any endogenous distribution shift. As introduced earlier, an endogenous distribution shift occurs when the environment, comprising reactive agents, changes in response to a shift in the ego agent's controller. We begin by formalizing a mathematical model for this distribution shift.

4.1. Modeling Endogenous Distribution Shift

Let \mathcal{Y} be the space of all possible trajectories and $\mathcal{P}(\mathcal{Y})$ be the set of all probability distributions on \mathcal{Y} . We can describe a metric space (\mathcal{Y}, W_1) , where W_1 is the 1-Wasserstein distance. We propose to capture the endogenous distribution shift through an iterative map $\mathcal{T}: \mathcal{P}(\mathcal{Y}) \to \mathcal{P}(\mathcal{Y})$ defined as

$$\mathcal{D}^{(r+1)} = \mathcal{T}(\mathcal{D}^{(r)}), \quad \text{where} \quad \mathcal{T} = F \circ CP. \tag{7}$$

Here, $\mathcal{D}^{(r)} \in \mathcal{P}(\mathcal{Y})$ is the distribution of interaction trajectories calibrated at iteration r, and $q^{(r)} = CP(\mathcal{D}^{(r)})$ is the uncertainty threshold obtained from CP applied to $\mathcal{D}^{(r)}$ (as detailed in Section 4.2). Effectively, the conformal prediction operator CP maps the trajectory distribution $\mathcal{D}^{(r)}$ to a statistically valid prediction error $q^{(r)}$, using a calibration dataset $D_{cal}^{(r)} := \{Y^{(r),1}, \dots, Y^{(r),K}\}$, where each trajectory $Y^{(r),i} \sim \mathcal{D}^{(r)}$. The mapping F is the new trajectory distribution induced by running $\pi_{MPC}(q^{(r)})$, as seen in Equation 5. Thus, \mathcal{T} models the combined effect of uncertainty

^{2.} We may alternatively equip the metric space with another metric like the Total Variation Distance or the Kolmogorov–Smirnov (KS) metric.

quantification through CP and the resulting trajectory adaptations by the MPC planner. This formulation enables us to capture how the behaviors of other agents evolve in response to changes in the MPC controller of the ego agent. Our objective is to find a target controller π_{MPC}^* that induces no further distribution shift, i.e., $\mathcal{D}^* = \mathcal{T}(\mathcal{D}^*)$. In other words, if \mathcal{T} has a fixed point and show convergence of our end-to-end prediction and planning system to a unique fixed-point distribution \mathcal{D}^* , then we can find this stable solution and controller using an iterative algorithm.

Assumption 1 (Lipschitz Continuity of Conformal Prediction) The conformal prediction mapping CP is Lipschitz continuous w.r.t. the Wasserstein distance. There exists $L_{CP} \geq 0$ such that for any two trajectory distributions \mathcal{D}_1 and \mathcal{D}_2 ,

$$|CP(\mathcal{D}_1) - CP(\mathcal{D}_2)| \le L_{CP} W_1(\mathcal{D}_1, \mathcal{D}_2). \tag{8}$$

Remark 2 (Justification of Assumption 1) The above assumption relates to the shift of the quantile estimation process under changes in the underlying data distribution. The work (Aolaritei et al., 2025, Proposition 2.5) shows that if the score function $U: \mathcal{Y} \to \mathbb{R}$ is k-Lipschitz, then a data-space distribution shift translates to a corresponding shift in the distribution of the nonconformity scores. In (Aolaritei et al., 2025, Proposition 3.5), the authors provide an expression for the worst-case quantile and coverage using the parameters ϵ and ρ of the distribution shift. Thus, under mild assumptions, we can show that $L_{CP} \leq 1$.

Assumption 3 (Lipschitz Continuity of MPC) The MPC map F is Lipschitz continuous w.r.t. changes in the constraint set. There exists $L_{MPC} \geq 0$ such that for any two constraint sets q_1 and q_2 ,

$$W_1(F(q_1), F(q_2)) \le L_{MPC}|q_1 - q_2|.$$
 (9)

Remark 4 (**Justification of Assumption 3**) This assumption is about the sensitivity of the MPC's solution (the resulting trajectory distribution) to changes in the constraints. If the MPC cost function is strongly convex and the constraints vary smoothly (without abrupt switching), the optimal solution will change continuously with the parameters (locally) (Boot (1963); Cánovas and Parra (2025)).

Theorem 5 (Convergence to the fixed-point of the endogenous distribution shift map) If Assumptions 1 and 3 hold and the combined Lipschitz constant satisfies $\delta = L_{MPC} \cdot L_{CP} < 1$, then the operator $\mathcal{T} = F \circ CP$ is a contraction mapping on the space of trajectory distributions equipped with the Wasserstein metric, (\mathcal{Y}, W_1) . Consequently, the iteration $\mathcal{D}^{(r+1)} = \mathcal{T}(\mathcal{D}^{(r)})$ converges to a unique fixed-point distribution $\mathcal{D}^* = \lim_{r \to \infty} \mathcal{D}^{(r)}$.

Proof When we combine (8) and (9), we get,

$$W_1(\mathcal{T}(\mathcal{D}_1),\mathcal{T}(\mathcal{D}_2)) = W_1\Big(F\big(CP(\mathcal{D}_1)\big),F\big(CP(\mathcal{D}_2)\big)\Big) \leq L_{\mathrm{MPC}}.L_{\mathrm{CP}}\,W_1(\mathcal{D}_1,\mathcal{D}_2).$$

If $\delta = L_{\text{MPC}}.L_{\text{CP}} < 1$, we can guarantee convergence to a fixed-point by leveraging Banach's Fixed-Point Theorem (Banach (1922)). Hence, \mathcal{T} is a contraction mapping with $\mathcal{D}^* = \lim_{r \to \infty} \mathcal{D}^{(r)}$.

Since $\mathcal{D}^* = \mathcal{T}(\mathcal{D}^*)$, convergence of the distributions implies convergence of CP-based uncertainty predictions $q^{(r)}$ to q^* . This statistic can thus serve as a stopping criterion in practice. Thus, we now require the formulation for $q^{(r)}$.

4.2. Prediction Region Construction

We now describe how to construct a CP-based prediction to be utilized in the MPC planner (5). Given past observations, $(Y_0^{(r)},\ldots,Y_t^{(r)})$, TrajPred generates an H-step forecast, $(\hat{Y}_{t+1|t}^{(r)},\ldots,\hat{Y}_{t+H|t}^{(r)})$. During the calibration phase, for each iteration r, we form a dataset of K interaction trajectories, $D_{cal}^{(r)} \coloneqq \{Y^{(r),1},\ldots,Y^{(r),K}\}$ and $Y^{(r),i} \coloneqq \{Y^{(r),i}_0,Y^{(r),i}_1,\ldots\} \overset{\text{i.i.d.}}{\sim} \mathcal{D}^{(r-1)}$. For each i^{th} calibration trajectory $Y^{(r),i} \in D_{\text{cal}}$, and each horizon step κ , we define the nonconformity score,

$$U_{\kappa t}^{(r),i} = \|Y_{t+\kappa}^{(r),i} - \hat{Y}_{t+\kappa t}^{(r),i}\|_{2} \quad \forall \kappa \in \{1,\dots,H\}, \ i \in \{1,\dots,K\},$$
(10)

which measures the deviation between the predicted and ground truth state. We define the maximal nonconformity score across time and across all N agents,

$$U_{\kappa}^{(r),i} = \max_{t \in \{1,2,\dots\}} U_{\kappa|t}^{(r),i} \quad \forall \kappa \in \{1,\dots,H\}, \ i \in \{1,\dots,K\}.$$
(11)

The nonconformity scores that describe the maximal H-step prediction error across the entire trajectory, $\{U^{(r),i}\}_{i=1}^K$ are exchangeable. Assuming they are sorted in non-decreasing order, we can apply (2) at horizon κ , to obtain the threshold,

$$\hat{q}_{\kappa}^{(r)} = U_{\kappa}^{(r),p}, \qquad p = \lceil (1 - \epsilon)(K + 1) \rceil, \tag{12}$$

where, $\epsilon \in (0,1)$ is the failure probability. Hence we obtain $\hat{\boldsymbol{q}}^{(r)} \coloneqq [\hat{q}_1^{(r)},\ldots,\hat{q}_H^{(r)}]$ as the CP-based threshold such that it satisfies (1) in a new interaction, i.e.,

$$\mathbb{P}\left[\max_{t\in\{1,2,\dots\}}\left\|Y_{t+\kappa}^{(r),\text{test}}-\hat{Y}_{t+\kappa|t}^{(r),\text{test}}\right\|_{2}\leq \hat{q}_{\kappa}^{(r)}\right]\geq 1-\epsilon,\quad\forall\kappa\in\{1,\dots,H\},\ Y^{(r),\text{test}}\overset{\text{i.i.d.}}{\sim}\mathcal{D}^{(r-1)}.$$

We can utilize the above CP-based prediction set in the safety constraint of our MPC problem, i.e., $\pi_{\text{MPC}}(\hat{\boldsymbol{q}}^{(r)})$ which will ensure that the ego-agent plans safely using imperfect predictions with probability $1-\epsilon$ (Lindemann et al., 2023, Theorem 3). Our method is compatible with any CP-based frameworks such as those by Cauchois et al. (2024); Cleaveland et al. (2024).

4.3. Smoothing Filter for Prediction Set

As established in Section 4.1, at the fixed-point \mathcal{D}^* , we have a corresponding calibration threshold from CP given by q^* and a stable, fixed policy, $\pi_{MPC}(q^*)$. To ensure stable convergence to this fixed-point, we constrain the distribution shift over the iterations by applying a low-pass filter to the $\hat{q}^{(r)}$ update. This reduces the short-term fluctuations in the distribution shift across iterations.

We apply a smoothing filter on the prediction set update by filtering the calibration threshold. Given a new calibration threshold computed at iteration r, $\hat{q}^{(r+1)}$, using calibration data sampled from $\mathcal{D}^{(r)}$, the filtered threshold is given by,

$$q^{(r+1)} = (1-\gamma)q^{(r)} + \gamma \hat{q}^{(r+1)},$$
 (13)

where, $\gamma \in [0,1]$ is a hyperparameter to determine the extent of smoothness. This iterative smoothing serves to ensure that the induced trajectory distributions $\mathcal{D}^{(r)}$, corresponding to executing $\pi_{\mathrm{MPC}}(\boldsymbol{q}^{(r)})$, remain close to the preceding distributions $\mathcal{D}^{(r-1)}$. Thus, we constrain the system to evolve gradually and facilitate convergence to the fixed-point.

Algorithm 1 summarizes our iterative adaptation framework. Theorem 5 guarantees asymptotic convergence of Algorithm 1 to a fixed-point where, $\lim_{r\to\infty} ||q^{(r+1)} - q^{(r)}||_2 = 0$. However,

Algorithm 1 Iterative Conformal Prediction for Multi-Agent Interactive Systems

```
Require: Failure probability \epsilon, smoothing parameter \gamma, stopping criteria \phi, prediction horizon H

1: Initialize r \leftarrow 0; \boldsymbol{q}^{(0)} \leftarrow \boldsymbol{0}; p \leftarrow \lceil (K+1)(1-\epsilon) \rceil

2: repeat

3: Deploy \pi_{\mathrm{MPC}}(\boldsymbol{q}^{(r)}) with TrajPred to obtain predictions

4: Collect trajectories for D_{cal}^{(r)}

5: for \kappa from 1 to H do

6: U_{\kappa}^{(r,i)} \leftarrow \max_{t} \|Y_{t+\kappa}^{(r),i} - \hat{Y}_{t+\kappa}^{(r),i}\|_2 for each Y^{(r),i} \in D_{cal}^{(r)}

7: Apply (2) where \hat{q}_{\kappa}^{(r+1)} = U_{\kappa}^{(r),p}

8: end for

9: \boldsymbol{q}^{(r+1)} \leftarrow (1-\gamma).\boldsymbol{q}^{(r)} + \gamma.\hat{\boldsymbol{q}}^{(r+1)}

10: \Delta q = \|\hat{\boldsymbol{q}}^{(r+1)} - \boldsymbol{q}^{(r)}\|_2

11: r \leftarrow r + 1

12: until \Delta q \leq \phi

13: return \boldsymbol{q}^{(r)}
```

practical deployment in requires a stopping criterion to detect when steady state is approximately reached. We therefore consider the following stopping condition with a small constant ϕ^3 ,

$$\|\boldsymbol{q}^{(r+1)} - \boldsymbol{q}^{(r)}\|_{2} \le \phi.$$
 (14)

Hence, our framework described in Algorithm 1, is able to converge to a fixed-point, under the assumptions listed in Theorem 5, and guarantee probabilistic safety (with probability $1 - \epsilon$) of the MPC policy $\pi_{\text{MPC}}(q^*)$ in the presence of other reactive agents.

5. Results

In this section, we apply our iterative CP framework in two- and three-agent interactions. We consider that all agents can react to each other using the policy π_{MPC} where each agent makes trajectory predictions about the other agents based on past observations. The TrajPred method considered is a long short-term memory (LSTM) model trained on historical agent states, chosen for scalability with time-series data and limited training samples. Agents implement model predictive control (MPC) for collision avoidance, with the ego agent integrating CP uncertainty regions around other agents. Further details regarding the experimental setup is included in Appendix A.1. We compare four approaches:

- 1. No Conformal Prediction (NCP): No uncertainty quantification is applied, i.e., $\pi_{MPC}(0)$.
- 2. Baseline Conformal Prediction (BCP): Trajectories are collected from decentralized multiagent control with interactive agents. A trajectory predictor is fine-tuned on these trajectories (using $D_{tune}^{\rm BCP}$ trajectories), and a calibration dataset $D_{cal}^{\rm BCP}$ is constructed for uncertainty calibration once, i.e., r=1, similar to the method proposed by Lindemann et al. (2023).
- 3. **Iterative Conformal Prediction (ICP, Ours):** Utilizing the same fine-tuned predictor as BCP, the iterative CP framework is executed until convergence (14). For fairness, the total number of trajectories matches that of BCP but is distributed across iterations, i.e., $|D_{cal}^{\rm BCP}| = r.K$.
- 3. For simplicity, we have considered the interaction between two agents, i.e., N=1, but note that we can apply the same updates for all non-ego agent (N>1) individually. We update the stopping criteria to $\max_{j\in\{0,\dots,N\}}\|\boldsymbol{q}_i^{(r+1)}-\boldsymbol{q}_i^{(r)}\|\leq\phi$.

Table 1: Performance metrics comparison for 2 Agents

Method	Collision	Deviation f	rom Ref. Path	Misdetection	Avg Nav	Success
	(in %)	Ego Agent	Other Agent	(in %)	Time(in s)	(in %)
NCP	43.00	0.12	0.12	_	6.10	57.00
BCP	0.00	0.63	0.08	0.30	7.64	90.50
ICP*	0.50	0.32	0.08	12.35	6.67	96.50
ISCP*	1.50	0.29	0.08	4.10	6.83	97.00

4. **Iterative Split Conformal Prediction (ISCP, Ours):** The Iterative Split Conformal Prediction framework is based on split-conformal prediction as shown in Tibshirani (2023) where the predictor is retrained and prediction sets are calibrated iteratively. The predictor is trained with a dataset size as the predictor trained in BCP, i.e, $|D_{tune}^{BCP}| = r.K_{tune}$ and $|D_{cal}^{BCP}| = r.K$. This framework is applied until the convergence criteria (14) is satisfied.

5.1. Two Agent Simulations

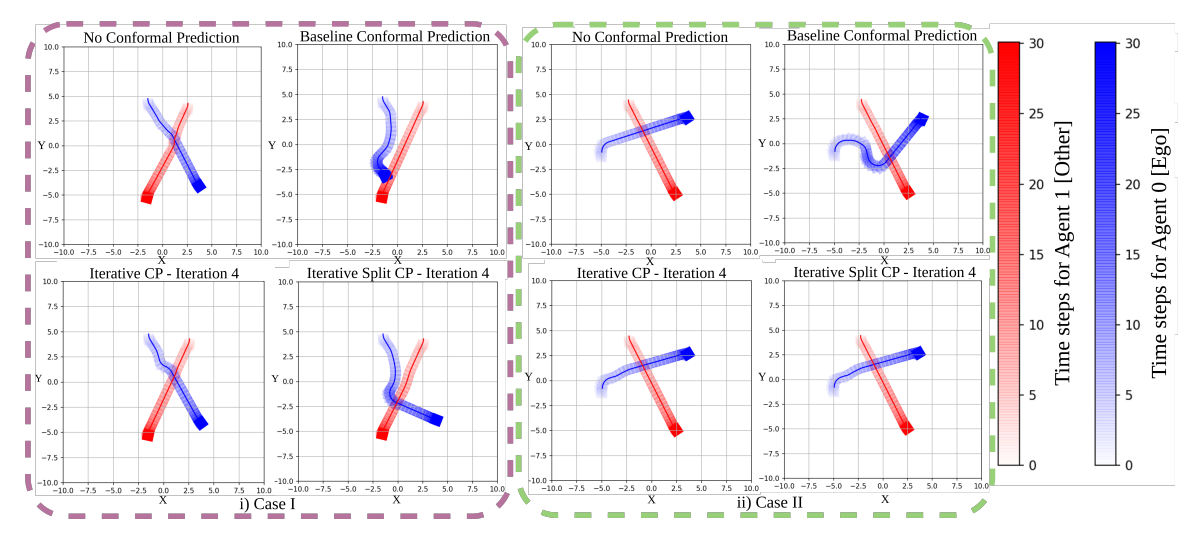


Figure 2: *Comparison for 2 agents across test cases*: Our iterative methods produce trajectories closely matching those without conformal prediction. In Case I, the baseline conformal prediction (BCP) method leads to a deadlock, while in Case II, BCP exhibits significant trajectory deviation.

We consider a two-agent scenario where the ego agent employs conformal prediction while the other agent uses a nominal MPC controller without uncertainty quantification, *i.e.*, $\pi_{\text{MPC}}(\mathbf{0})$. For conformal prediction, following (3) the failure (and misdetection) probability $\epsilon = 0.15$ with $\delta = 0.01$. The smoothing parameter $\gamma = 0.8$ for ICP and $\gamma = 0.9$ for ISCP, and the stopping criteria $\phi = 0.1$. For both baseline conformal prediction (BCP) and ICP, the predictor is trained on $|D_{tune}^{\text{BCP}}| = 1000$ trajectories and with $|D_{cal}^{\text{BCP}}| = 1000$. The ICP method uses K = 250 for each iteration. For ISCP, $K_{tune} = 250$, K = 250 trajectories are used per iteration for retraining the predictor and calibration respectively. The ISCP method converges in r = 4 iterations while the ICP method converges in r = 4 iterations. Please refer to Appendix A.3 for further details.

We use 200 test trajectories for obtaining the results reported in Table 1 (the evaluation metrics used are explained in Appendix A.2). The results show NCP leads to most collisions and unsafe

Table 2: Performance metrics comparison for 3 Agents

Method	Collision	Deviation f	rom Ref. Path	Misdetection	Avg Nav	Success	
	(in %)	Ego Agent	Other Agent	(in %)	Time(in s)	(in %)	
NCP	35.17	0.17	0.23	_	8.72	24.50	
BCP	2.33	0.65	0.72	40.40	11.04	88.50	
ICP*	1.00	1.04	1.25	11.03	13.29	87.50	
ISCP*	0.00	0.49	0.50	7.10	11.90	97.00	

behavior, while BCP, which does not split the calibration budget into iterations and uses the entire budget in one iteration, exhibits overly conservative behavior with larger ego-agent path deviations and reduced success rates due to deadlocks, as demonstrated in Fig. 2. In contrast, our ICP method adaptively updates the agent behavior towards a stable configuration, resulting in reduced deviations from the reference trajectory while still satisfying the desired safety levels. Moreover, our ISCP method, which retrains the predictor alongside iterative calibration, yields higher success rates, smaller ego-agent path deviations, and also maintains misdetections within the target bounds.

5.2. Three Agent Simulations

We consider a three-agent scenario in which all agents, in contrast to the two-agent setting discussed in Section 5.1, incorporate CP-based uncertainty predictions within their MPC planners. We use the misdetection probability $\epsilon=0.10$ with $\delta=0.01$, $\gamma=0.9$, and $\phi=0.2$. For BCP, $|D_{tune}^{\rm BCP}|=1000$ and $|D_{cal}^{\rm BCP}|=1000$. The ICP uses K=250 for each iteration for calibration and ISCP uses $K_{tune}=250$ and K=250. The ICP and ISCP methods converge in r=4 iterations. However, we note that if we run ICP for more iterations, the prediction sets start changing again, indicating that the fixed-point for ICP is unstable. Please see Appendix A.4 for more details and experiments.

The results, summarized in Table 2, demonstrate that BCP, now overly optimistic in its behavior, fails to meet the desired misdetection coverage. This behavior contrasts with the two-agent case. In both cases, the unmodeled distribution shift causes the baseline to be either too optimistic or too conservative. When we instead split the budget across multiple iterations, both ICP and ISCP show better performance by satisfying the desired collision guarantees. We see that much like the 2-agent case, ISCP gives us improved performance across most metrics.

6. Conclusion and Future Work

We introduce an iterative CP framework for multi-agent reactive systems under endogenous distribution shift. By iteratively recalibrating prediction regions, the proposed method achieves desired coverage guarantees while adapting to the distribution shift. We note, however, that the use of smoothing filters for prediction sets requires some hyperparameter tuning. Future research will focus on developing adaptive strategies to mitigate hyperparameter sensitivity and exploring alternative statistical techniques beyond CP to describe the endogenous distribution shift such as using the statistical properties inherent to certain generative learning modules. Finally, we seek to deploy the theory presented on physical robotic platforms for real-world applications.

Acknowledgments

The authors would like to thank Debajyoti Chakrabarti for his valuable insights and Professor Saumik Bhattacharya for supporting the inclusion of this work in the author's Master's thesis.

References

- Alexandre Alahi, Kratarth Goel, Vignesh Ramanathan, Alexandre Robicquet, Li Fei-Fei, and Silvio Savarese. Social lstm: Human trajectory prediction in crowded spaces. In 2016 IEEE Conference on Computer Vision and Pattern Recognition (CVPR), pages 961–971, 2016. doi: 10.1109/CVPR. 2016.110.
- Aaron D. Ames, Xiangru Xu, Jessy W. Grizzle, and Paulo Tabuada. Control barrier function based quadratic programs for safety critical systems. *IEEE Transactions on Automatic Control*, 62(8): 3861–3876, 2017. doi: 10.1109/TAC.2016.2638961.
- Joel A E Andersson, Joris Gillis, Greg Horn, James B Rawlings, and Moritz Diehl. CasADi A software framework for nonlinear optimization and optimal control. *Mathematical Programming Computation*, 11(1):1–36, 2019. doi: 10.1007/s12532-018-0139-4.
- Anastasios N. Angelopoulos and Stephen Bates. A gentle introduction to conformal prediction and distribution-free uncertainty quantification, 2022. URL https://arxiv.org/abs/2107.07511.
- Anastasios N. Angelopoulos, Stephen Bates, Adam Fisch, Lihua Lei, and Tal Schuster. Conformal risk control, 2025. URL https://arxiv.org/abs/2208.02814.
- Liviu Aolaritei, Zheyu Oliver Wang, Julie Zhu, Michael I. Jordan, and Youssef Marzouk. Conformal prediction under levy-prokhorov distribution shifts: Robustness to local and global perturbations, 2025. URL https://arxiv.org/abs/2502.14105.
- Stefan Banach. Sur les opérations dans les ensembles abstraits et leur application aux équations intégrales. *Fundamenta Mathematicae*, 3:133–181, 1922.
- John CG Boot. On sensitivity analysis in convex quadratic programming problems. *Operations Research*, 11(5):771–786, 1963.
- Maxime Cauchois, Suyash Gupta, Alnur Ali, and John C. Duchi. Robust validation: Confident predictions even when distributions shift. *Journal of the American Statistical Association*, 119 (548):3033–3044, February 2024. ISSN 1537-274X. doi: 10.1080/01621459.2023.2298037. URL http://dx.doi.org/10.1080/01621459.2023.2298037.
- Kan Chen, Runzhou Ge, Hang Qiu, Rami Ai-Rfou, Charles R. Qi, Xuanyu Zhou, Zoey Yang, Scott Ettinger, Pei Sun, Zhaoqi Leng, Mustafa Mustafa, Ivan Bogun, Weiyue Wang, Mingxing Tan, and Dragomir Anguelov. Womd-lidar: Raw sensor dataset benchmark for motion forecasting. In *Proceedings of the IEEE International Conference on Robotics and Automation (ICRA)*, May 2024.
- Matthew Cleaveland, Insup Lee, George J. Pappas, and Lars Lindemann. Conformal prediction regions for time series using linear complementarity programming, 2024. URL https://arxiv.org/abs/2304.01075.
- M. Cánovas and Juan Parra. Lipschitz stability in convex optimization. *Set-Valued and Variational Analysis*, 33, 07 2025. doi: 10.1007/s11228-025-00760-8.

- Anushri Dixit, Lars Lindemann, Skylar X Wei, Matthew Cleaveland, George J. Pappas, and Joel W. Burdick. Adaptive conformal prediction for motion planning among dynamic agents. In Nikolai Matni, Manfred Morari, and George J. Pappas, editors, *Proceedings of The 5th Annual Learning for Dynamics and Control Conference*, volume 211 of *Proceedings of Machine Learning Research*, pages 300–314. PMLR, 15–16 Jun 2023. URL https://proceedings.mlr.press/v211/dixit23a.html.
- Alexey Dosovitskiy, German Ros, Felipe Codevilla, Antonio Lopez, and Vladlen Koltun. CARLA: An open urban driving simulator. In *Proceedings of the 1st Annual Conference on Robot Learning*, pages 1–16, 2017.
- Ashligh Fields. San francisco leaders call for new checks on waymo after death of beloved cat kitkat, 2025. URL https://thehill.com/policy/energy-environment/5591776-san-francisco-waymo-regulation-cat/.
- D. Fox, W. Burgard, and S. Thrun. The dynamic window approach to collision avoidance. *IEEE Robotics and Automation Magazine*, 4(1):23–33, 1997. doi: 10.1109/100.580977.
- Sepp Hochreiter and Jürgen Schmidhuber. Long short-term memory. *Neural Computation*, 9(8): 1735–1780, 1997. doi: 10.1162/neco.1997.9.8.1735.
- Tom Kuipers, Renukanandan Tumu, Shuo Yang, Milad Kazemi, Rahul Mangharam, and Nicola Paoletti. Conformal off-policy prediction for multi-agent systems. In 2024 IEEE 63rd Conference on Decision and Control (CDC), pages 1067–1074, 2024. doi: 10.1109/CDC56724.2024. 10886791.
- Lars Lindemann, Matthew Cleaveland, Gihyun Shim, and George J. Pappas. Safe planning in dynamic environments using conformal prediction. *IEEE Robotics and Automation Letters*, 8(8): 5116–5123, 2023. doi: 10.1109/LRA.2023.3292071.
- Zhiting Mei, Anushri Dixit, Meghan Booker, Emily Zhou, Mariko Storey-Matsutani, Allen Z. Ren, Ola Shorinwa, and Anirudha Majumdar. Perceive with confidence: Statistical safety assurances for navigation with learning-based perception, 2025. URL https://arxiv.org/abs/2403.08185.
- R. Pepy, A. Lambert, and H. Mounier. Path planning using a dynamic vehicle model. In 2006 2nd International Conference on Information and Communication Technologies, volume 1, pages 781–786, 2006. doi: 10.1109/ICTTA.2006.1684472.
- Juan Perdomo, Tijana Zrnic, Celestine Mendler-Dünner, and Moritz Hardt. Performative prediction. In Hal Daumé III and Aarti Singh, editors, *Proceedings of the 37th International Conference on Machine Learning*, volume 119 of *Proceedings of Machine Learning Research*, pages 7599–7609. PMLR, 13–18 Jul 2020. URL https://proceedings.mlr.press/v119/perdomo20a.html.
- Nicholas Rhinehart, Rowan Mcallister, Kris Kitani, and Sergey Levine. Precog: Prediction conditioned on goals in visual multi-agent settings. In *2019 IEEE/CVF International Conference on Computer Vision (ICCV)*, pages 2821–2830, 2019. doi: 10.1109/ICCV.2019.00291.

- Tim Salzmann, Boris Ivanovic, Punarjay Chakravarty, and Marco Pavone. Trajectron++: Dynamically-feasible trajectory forecasting with heterogeneous data, 2021. URL https://arxiv.org/abs/2001.03093.
- Sepehr Samavi, Anthony Lem, Fumiaki Sato, Sirui Chen, Qiao Gu, Keijiro Yano, Angela P. Schoellig, and Florian Shkurti. Sicnav-diffusion: Safe and interactive crowd navigation with diffusion trajectory predictions. *IEEE Robotics and Automation Letters*, 10(9):8738–8745, 2025. doi: 10.1109/LRA.2025.3585713.
- Shaoshuai Shi, Li Jiang, Dengxin Dai, and Bernt Schiele. Motion transformer with global intention localization and local movement refinement. *Advances in Neural Information Processing Systems*, 2022.
- Ryan Tibshirani. Conformal prediction. Lecture notes, Advanced Topics in Statistical Learning, Spring 2023, UC Berkeley, 2023. URL https://www.stat.berkeley.edu/~ryantibs/statlearn-s23/lectures/conformal.pdf.
- Vladimir Vovk. Conditional validity of inductive conformal predictors. In Steven C. H. Hoi and Wray Buntine, editors, *Proceedings of the Asian Conference on Machine Learning*, volume 25 of *Proceedings of Machine Learning Research*, pages 475–490, Singapore Management University, Singapore, 04–06 Nov 2012. PMLR. URL https://proceedings.mlr.press/v25/vovk12.html.
- Vladimir Vovk, Alex Gammerman, and Glenn Shafer. *Algorithmic Learning in a Random World*. Springer-Verlag, Berlin, Heidelberg, 2005. ISBN 0387001522.
- Ye Yuan, Xinshuo Weng, Yanglan Ou, and Kris Kitani. Agentformer: Agent-aware transformers for socio-temporal multi-agent forecasting, 2021. URL https://arxiv.org/abs/2103.14023.

Appendix A. Experimental Details

A.1. Additional Details on System Dynamics and Environment

For all the experiments, we consider the bicycle model (Pepy et al. (2006)):

$$\begin{bmatrix} x_{t+1} \\ y_{t+1} \\ \theta_{t+1} \\ v_{t+1} \end{bmatrix} = \begin{bmatrix} x_t + \Delta v_t \cos(\theta_t) \\ y_t + \Delta v_t \sin(\theta_t) \\ \theta_t + \frac{\Delta v_t}{l} \tan(\phi_t) \\ v_t + \Delta a_t \end{bmatrix}$$
(15)

where $p_t \coloneqq (x_t, y_t)$ denotes the position in 2-dimensional cartesian-plane, θ_t is the vehicle's orientation, v_t is the velocity of the vehicle, $l \coloneqq 1$ is the vehicle's length and $\Delta \coloneqq 0.1s$ is the sampling time. The control inputs for this model are ϕ_t , which denotes the steering angle, and a_t , which denotes the acceleration of the vehicle.

In all the cases, the objective for the 0^{th} agent is to reach a goal region while avoiding the other reactive agents using the constraint function:

$$c(p_{t+\kappa|t}, \hat{Y}_{\kappa}) := \|p_{t+\kappa|t} - \hat{Y}_{\kappa,j}\| - \epsilon \tag{16}$$

Here, ϵ is the safe distance to be considered between the agents. While this formulation has been defined for the ego-agent, it is extended to all the other agents as well, with the constraint to avoid all the other agents, including the ego-agent. The center of the goal region is considered as x_g with zero velocity at goal point, *i.e.*, $v_g = 0$.

The MPC Cost Function J(.), which we define for the experiments, is the standard goal-reaching MPC formulation as shown:

$$J(x_{\tau}, u_{\tau}) := (x_{\tau} - x_g)^T Q(x_{\tau} - x_g) + u_{\tau}^T R u_{\tau} + 0.01 * v_{\tau}$$
(17)

where, Q = diag([1, 1, 0.001, 0.1]) and R = diag([0.001, 0.01]). Here, diag([.]) is used to represent a diagonal matrix whose diagonal elements are provided. We also consider a terminal constraint $(Q_T = diag([5.0, 5.0, 0.01, 5.5]))$. To solve the MPC optimization problem, we use CasADi (Andersson et al. (2019)) with Ipopt non-linear programming solver.

A.2. Evaluation Metrics

The evaluation metrics used in Table 1 and 2 are explained below:

- 1. **Collision Rate:** Percentage of trajectories in which at least one agent experiences a collision at any time, measuring the safety of the conformal prediction framework.
- 2. Misdetection: Percentage of prediction instances where the ground-truth position of the agent lies outside the CP-based uncertainty set, computed across all agents, prediction horizons, and test samples, assessing the statistical validity of the uncertainty quantification. This metric provides a measure of the extent of distributional shift that occurs when the misdetection rate computed from the test trajectories varies from the misdetection rate imposed by the calibration dataset.

- 3. **Success Rate:** The percentage of trajectories in which the ego agent successfully reaches its designated goal within the specified time limit of 30 seconds and in which no collision occurs throughout the entire trajectory. This metric captures the effectiveness of the conformal prediction framework to avoid collisions and simultaneously to ensure over-conservativeness of the CP-based prediction frameworks, leading to overly conservative prediction regions.
- 4. **Average Navigation Time:** The mean time taken by the agents that use CP-based methods to reach their goal position for all the successful attempts. Unsuccessful attempts are not considered in this calculation.
- 5. **Deviation from Reference Path:** The deviation of the agents' actual trajectories from their nominal reference paths. This metric quantifies the size of the CP-based uncertainty predictions by measuring the distance between the executed trajectories and the planned reference.

A.3. Additional Details for Two Agent Simulations

In the two-agent environment, initial positions and goal locations are randomly initialized on a circle of diameter 10, with a bias towards diagonal opposition and random displacement, subject to a minimum distance constraint to prevent initial collisions. This simulation setup ensures diverse, non-overlapping start and end configurations for both agents.

For the Iterative Split Conformal Prediction (ISCP) framework, iteration 0 begins with agents ignoring other agents, leading to frequent collisions, and serves as a base case for predictor training. In the Table 3, we show how the performance metrics vary over iterations. Table 3 summarizes performance metrics over ISCP iterations, showing adaptation of the CP-based uncertainty sets to improve success rates and reduce path deviation, while maintaining statistical guarantees. Table 4 records misdetection rates for each prediction step across iterations.

T 11 0 D C		• ,	C .1	TOOD	1
Table 3: Performance	metrice	Over iterations	Of the	1000	ramework
Table 9. I CHOHIIIance	HICHICS	Over neralions	OI LIIC	. 1030-1	ianicwoik

Iteration	Collision	Deviation for	rom Ref. Path	Misdetection	Avg Nav	Success	
r	(in %)	Ego Agent	Other Agent	(in %)	Time(in s)	(in %)	
0	0.00	0.00	-	-	5.80	20.00	
1	3.00	0.56	0.11	16.00	7.10	88.00	
2	1.00	0.45	0.09	5.90	7.20	93.50	
3	0.50	0.40	0.07	3.00	6.89	94.50	
4	1.50	0.29	0.08	4.10	6.83	97.00	

Table 4: Misdetection Rate for 2 Agents of ISCP over H=10 prediction steps

r	All Steps	Step 1	Step 2	Step 3	Step 4	Step 5	Step 6	Step 7	Step 8	Step 9	Step 10
1	16.00	14.50	15.50	14.50	13.50	15.50	17.50	16.50	17.50	17.50	17.50
2	5.90	6.00	5.50	5.00	5.00	5.00	6.00	6.00	6.50	7.00	7.00
3	3.00	4.00	1.50	2.00	2.50	3.00	3.50	3.00	3.50	3.50	3.50
4	4.10	3.50	4.00	5.00	4.50	4.00	4.00	4.00	4.00	4.00	4.00

For the Iterative Conformal Prediction (ICP) framework, agents at iteration 0 plan collisionfree trajectories without CP-based uncertainty predictions (i.e., with $q^{(r)} = 0$). Table 5 presents corresponding performance metrics across ICP iterations, while Table 10 reports misdetections. Notably, the misdetection rate is generally higher for ICP compared to ISCP, as tighter uncertainty sets are calibrated from available predictor outputs.

Table 5: Performance metrics over iterations of the ICP framework

Iteration	Collision	Deviation for	rom Ref. Path	Misdetection	Avg Nav	Success	
r	(in %)	Ego Agent	Other Agent	(in %)	Time(in s)	(in %)	
0	42.50	0.13	0.12	_	6.04	57.50	
1	0.00	0.59	0.09	0.20	7.56	92.00	
2	6.50	0.30	0.08	16.60	6.68	90.50	
3	2.50	0.36	0.08	12.25	6.78	93.50	
4	0.50	0.32	0.08	12.35	6.67	96.50	

Table 6: Misdetection Rate for 2 Agents of ICP over H=10 prediction steps

r	All Steps	Step 1	Step 2	Step 3	Step 4	Step 5	Step 6	Step 7	Step 8	Step 9	Step 10
1	0.20	0.00	0.0	0.0	0.0	0.50	1.00	0.50	0.0	0.0	0.0
2	16.60	14.50	17.50	17.50	17.50	18.00	16.50	16.00	16.00	16.00	16.50
3	12.25	9.00	11.00	12.00	12.50	12.50	13.00	12.50	13.00	13.50	13.50
4	12.35	9.50	12.00	13.00	13.00	12.00	12.50	12.50	13.00	13.00	13.00

Plots of CP-based uncertainty predictions $q^{(r)}$ over the prediction horizon for ISCP and ICP are shown in Figure 5.

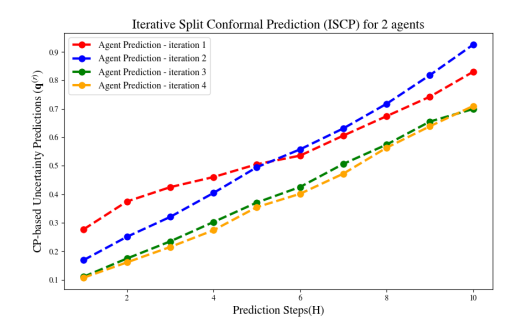


Figure 3: ISCP: $q^{(r)}$ over H

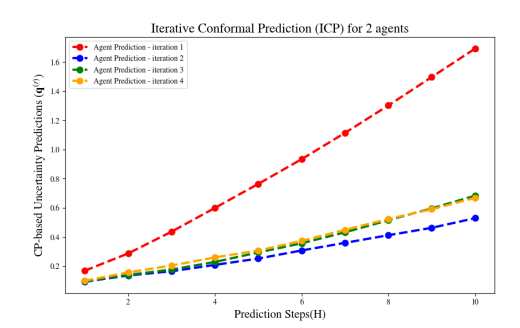


Figure 4: ICP: $q^{(r)}$ over H

Figure 5: CP-based uncertanity predictions for 2 agents

A.4. Additional Details for Three Agent Simulations

The initial and goal points are obtained in a similar manner as explained in A.3. We, however, consider the diameter of the circle as 15 to accommodate more agents.

In the Table 7, we show how the performance metrics vary over iterations when all the agents deploy the MPC planner with CP-based uncertainty predictions. We observe that over iterations,

the CP-based uncertainty sets update to increase the success rate and reduce deviations, while maintaining statistical guarantees. In Table 4, we notice how the mis-detections (in %) change over the iterations for each of the H prediction steps.

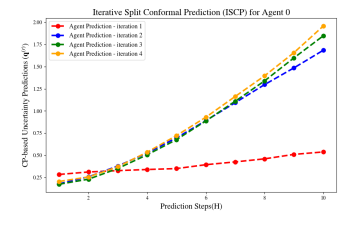
Table 7: Performance metrics over iterations of the ISCP framework

Iteration	Collision	Deviation f	rom Ref. Path	Misdetection	Avg Nav	Success	
r	(in %)	Ego Agent	Other Agent	(in %)	Time(in s)	(in %)	
0	58.17	0.00	0.00	_	7.31	19.50	
1	5.83	0.31	0.28	71.25	9.72	88.00	
2	0.33	0.64	0.52	26.80	13.06	91.00	
3	0.00	0.72	0.57	12.25	12.30	96.50	
4	0.00	0.49	0.50	7.10	11.90	97.00	

Table 8: Misdetection Rate for 3 Agents of ISCP over H=10 prediction steps

r	All Steps	Step 1	Step 2	Step 3	Step 4	Step 5	Step 6	Step 7	Step 8	Step 9	Step 10
1	71.25	32.83	40.17	50.67	62.17	75.50	82.00	88.00	92.83	94.00	94.33
2	26.80	19.50	25.50	28.67	31.50	31.50	27.00	25.33	25.83	26.50	26.67
3	12.25	8.50	13.67	13.67	14.50	15	12.83	11.67	10.83	10.67	11.17
4	7.10	1.83	5.00	5.50	6.50	7.33	8.67	8.67	8.50	9.50	9.50

From the Figure 21, we observe the converging behavior for the CP-based uncertainty sets with the ISCP framework where $\gamma=0.9$. We observe that the predictor and the CP-based uncertainty sets converge to a more stable behavior for all the agents, with misdetection coverage guarantees satisfied.



Age Productors Support

Age Pr

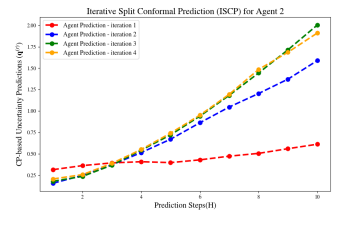


Figure 6: Agent 0

Figure 7: Agent 1

Figure 8: Agent 2

Figure 9: ISCP: CP-based Uncertainty Predictions over Prediction Steps for 3 agents

Table 9 reports the performance metrics of the ICP framework over multiple iterations for a 3-agent environment. The CP-based uncertainty sets, $q^{(r)}$, adapt progressively to increase the success rate while aiming to satisfy the required misdetection coverage. Notably, iteration 2 achieves the targeted misdetection coverage with an improved success rate and reduced collision frequency. Subsequent iterations maintain comparable performance, though slight fluctuations in deviation and misdetection rates are observed.

Table 9: Performance metrics over iterations of the ICP framework for 3 agents

Iteration	Collision	Deviation for	rom Ref. Path	Misdetection	Avg Nav	Success	
r	(in %)	Ego Agent	Other Agent	(in %)	Time(in s)	(in %)	
0	32.83	0.16	0.21	-	8.65	27.50	
1	2.00	0.81	0.76	40.90	13.37	87.50	
2	1.50	0.86	0.99	9.78	12.94	89.50	
3	2.33	1.10	0.96	11.90	15.00	81.00	
4	1.00	1.04	1.25	11.03	13.29	87.50	

Table 10: Misdetection Rate for 3 Agents of ICP over H = 10 prediction steps

r	All Steps	Step 1	Step 2	Step 3	Step 4	Step 5	Step 6	Step 7	Step 8	Step 9	Step 10
1	40.90	34.67	34.50	36.00	37.17	40.33	43.67	44.17	45.83	46.17	46.50
2	9.78	9.17	9.67	9.00	8.83	9.00	10.00	10.83	10.50	10.83	10.00
3	11.90	11.50	12.00	12.00	12.00	11.67	12.00	12.00	13.33	11.67	10.83
4	11.03	12.50	12.67	12.00	11.50	11.17	11.00	10.83	9.83	9.50	9.33

We investigate the effect of varying the smoothing parameter, considering $\gamma=0.2,0.8,0.9$. For each setting, the iterative procedure is executed for several steps beyond the predefined stopping criterion. The results indicate that the CP-based uncertainty predictions $\boldsymbol{q}^{(r)}$ approach a convergent value \boldsymbol{q}^* but exhibit oscillatory behavior as iterations progress past the stopping condition. This phenomenon is particularly pronounced for larger values of γ , corresponding to lower smoothing. The convergence towards the stopping criterion typically occurs around iteration 4; however, subsequent iterations lead to increased divergence in the uncertainty sets. As mentioned earlier, iteration 2 achieves the optimal balance, with minimal collisions and elevated success rates, as well as satisfying the targeted coverage. Notably, most of the $\boldsymbol{q}^{(r)}$ are found to adapt to values near $\boldsymbol{q}^{(2)}$ which might indicate a fixed-point.

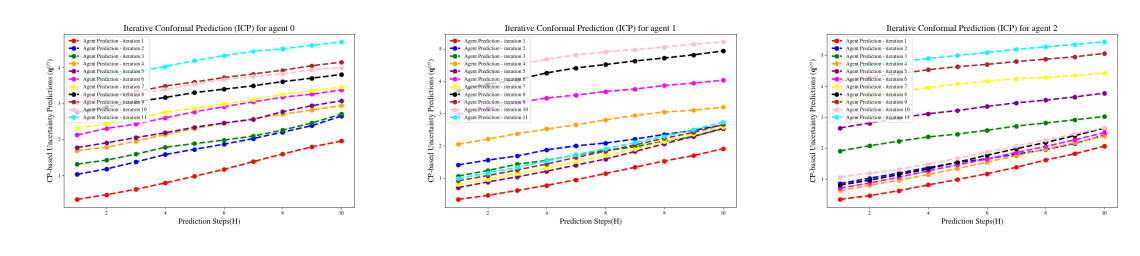


Figure 13: ICP($\gamma = 0.9$): CP-based Uncertainty Predictions over Prediction Steps for 3 agents

Figure 11: Agent 1

Figure 12: Agent 2

Figure 10: Agent 0

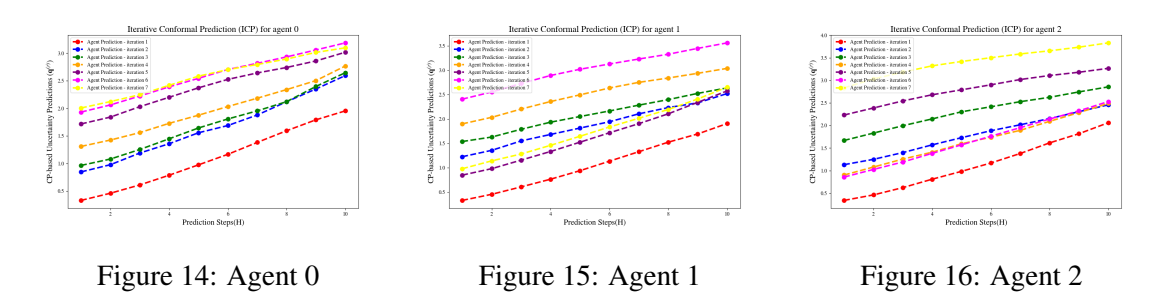


Figure 17: ICP($\gamma = 0.8$): CP-based Uncertainty Predictions over Prediction Steps for 3 agents

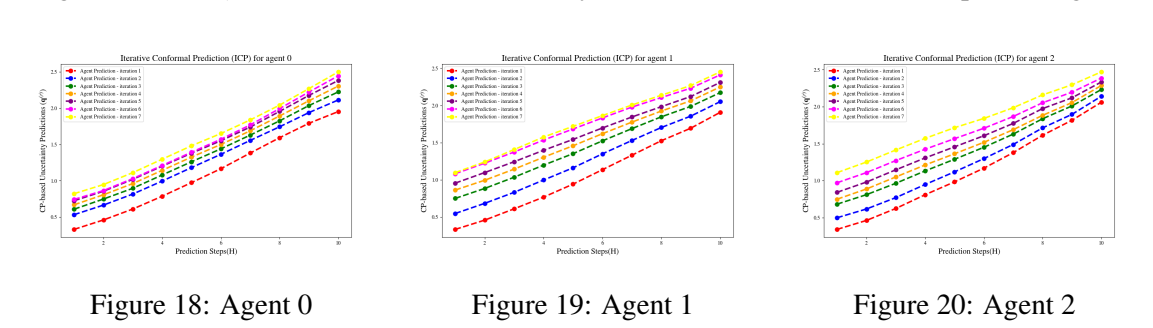


Figure 21: ICP($\gamma = 0.2$): CP-based Uncertainty Predictions over Prediction Steps for 3 agents